



HAL
open science

Early moments of BLEVE: From vessel opening to liquid flashing release

A.M. Birk, R. Eyssette, F. Heymes

► To cite this version:

A.M. Birk, R. Eyssette, F. Heymes. Early moments of BLEVE: From vessel opening to liquid flashing release. *Process Safety and Environmental Protection*, 2019, 132, pp.35-46. 10.1016/j.psep.2019.09.028 . hal-02428264

HAL Id: hal-02428264

<https://imt-mines-ales.hal.science/hal-02428264>

Submitted on 28 Jul 2020

HAL is a multi-disciplinary open access archive for the deposit and dissemination of scientific research documents, whether they are published or not. The documents may come from teaching and research institutions in France or abroad, or from public or private research centers.

L'archive ouverte pluridisciplinaire **HAL**, est destinée au dépôt et à la diffusion de documents scientifiques de niveau recherche, publiés ou non, émanant des établissements d'enseignement et de recherche français ou étrangers, des laboratoires publics ou privés.

Early moments of BLEVE: From vessel opening to liquid flashing release

A.M. Birk^a, R. Eyssette^{a,b,*}, F. Heymes^b

^a Department of Mechanical and Materials Engineering, Queen's University, Kingston, Ontario, Canada

^b LGEI, IMT Mines Alès, Alès, France

A B S T R A C T

The boiling liquid expanding vapour explosion (BLEVE) is well known but not well understood. Some still argue about what comes first, the BLEVE or the vessel rupture. Some believe the BLEVE is triggered by some pressure transient inside the vessel and this causes a superheat limit explosion which causes the vessel to rupture. Others believe it is the vessel rupture by some weakening process that leads to the BLEVE. This paper will provide evidence that the latter description that is correct for most, if not all BLEVEs observed in practice.

This paper describes small scale experiments of aluminum tubes that were weakened by machining a thinned wall area over a specified length. The tubes were filled to a desired level with liquid propane and then the propane was uniformly heated electrically until the tubes failed. The failure pressures ranged from 10 to 33 bar.

The tube was instrumented to capture failure characteristics (pressure, temperature) and consequences: blast overpressure and imaging of the propane cloud and shock around the vessel; ground force under it; transient pressure and imaging of the boiling process inside the vessel. The work was done to improve our understanding of the fluid – structure interactions during the fire heat induced failure of a pressure vessel holding a pressure liquefied gas. We were specifically interested in the near field hazards including blast overpressure and ground force. This paper will focus on the early milliseconds of the process where the vessel begins to open and a shock wave is formed and moves out into the surroundings. The imaging reveals presence of a Mach shock at the exit of the vessel at the early stage of the opening. A chronology of the event also shows that the lead shock is generated early in the explosion process, and is long gone before the liquid starts boiling, arguing that vapour expansion is the main contributor to the first shock overpressure.

Keywords:

BLEVE

Boiling liquid expanding vapor explosion

Explosion

Overpressure

Experimental results

High speed imaging

Timeline analysis

Lead shock

Explosive phase change

1. Introduction

1.1. Background and motivation

The Boiling Liquid Expanding Vapor (BLEVE) is a feared accident in the industry. Many cases have been reported over the past 60 years throughout the world (Hemmatian et al., 2019). Their consequences are often deadly and very destructive for the surrounding structures. There has been a lot of studies on the multiple hazards this accident generates to understand it better and predicted its consequences (Abbasi and Abbasi, 2007; Eckhoff, 2014). However, models to predict these hazards consequences are based on diverg-

ing interpretations of the physics of the phenomenon (Laboureur et al., 2014). This work aims at refining our understanding of the different physical phenomena involved in a BLEVE.

The definition of BLEVE has evolved through the years with our understanding of it. In this paper we use the following definition of a BLEVE (Birk et al., 2007) “the explosive release of expanding vapour and flashing liquid when a pressure vessel holding a pressure liquefied gas fails catastrophically”

From this definition a BLEVE requires

- i) an explosion which suggests a supersonic shock wave is sent into the surroundings
- ii) a pressure liquefied gas must be present to generate a rapid phase change event
- iii) the vessel must fail catastrophically and open fully to release its contents

* Corresponding author at: Department of Mechanical and Materials Engineering, Queen's University, Kingston, Ontario, Canada.

E-mail address: eysssette.roland@queensu.ca (R. Eyssette).

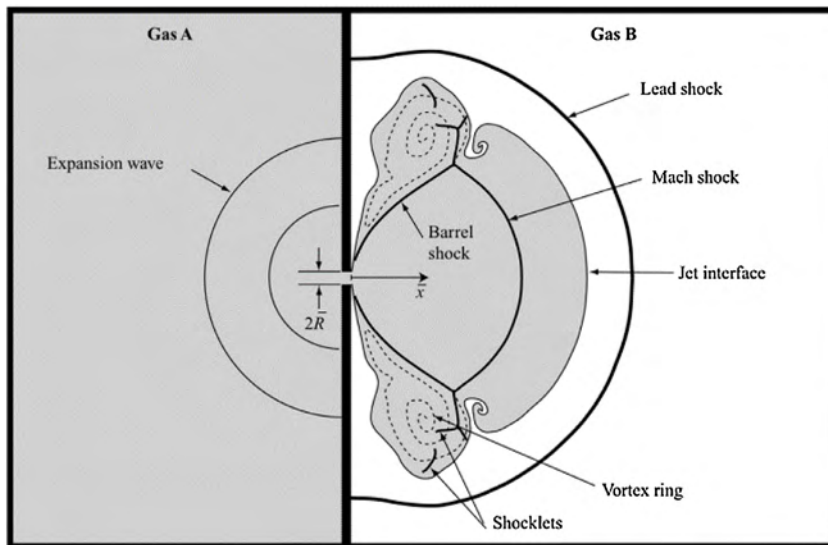


Fig. 1. the starting of a lead shock from the transient flow from an opening in a pressurized container (from Radulescu and Law, 2007).

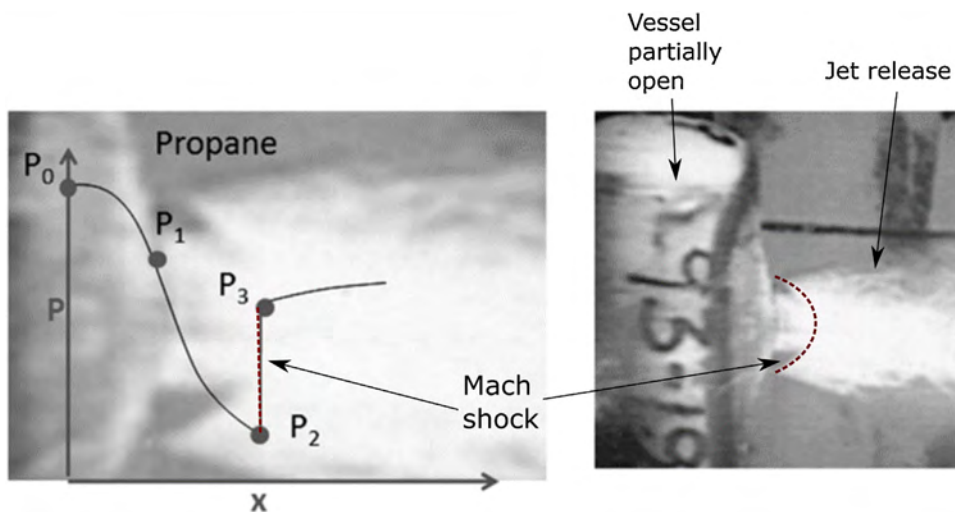


Fig. 2. Pressure Distribution along axis of fish mouth opening on vessel with image of jet showing Mach shock standing beyond opening (vessel $D = 0.61$ m, propane, failure pressure approximately 20 Barg) (Laboureur et al., 2015).

There is no mention of the atmospheric superheat limit in this definition, as mentioned in older definitions. We will come back to this point later in this paper.

There is a current need to understand the near field hazards from a BLEVE. The most recent BLEVE in the news was one on a bridge in Bologna Italy in 2018 (Vigilfuoco.tv, 2018). This tanker truck suffered a BLEVE and the load on the bridge caused the bridge deck to fail.

Over the years the authors have been asked by emergency responders what the near field effects are. These near field effects include the blast overpressure, ground loading, overpressure and drag loading from the flashing liquid, projectile effects and of course the fireball if the cloud is flammable. This paper will focus on the blast wave, liquid flashing and ground loading.

1.2. The vessel opening process

It is known from high speed imaging (Laboureur et al., 2015) that the vessel failure starts as a pin hole near the top of the vessel wall in the severely heated (weakened) area. In a single step BLEVE (Birk et al., 2007) this pin hole grows rapidly and continuously along

the vessel top in the axial direction, then it turns circumferentially at both ends of the weakened length. The pressure forces on the unsupported edges of the wall bend the vessel wall flaps up to open the vessel. The power of the expanding vapour and flashing liquid release usually opens the vessel completely and flattens the open vessel cylinder wall on the ground.

When the vessel is not fully filled with liquid, the opening initially sends out a high speed jet of vapour that pushes on the surrounding atmosphere like a piston. As the opening grows this jet grows in size and speed and the piston effect gets larger and stronger. A series of compression waves are sent out by the expanding jet cloud and the following compression waves catch up with the leading waves to produce a shock wave. This shock wave grows to full strength at some distance from the vessel wall. The distance from the wall and the shock strength depend on how quickly the vessel opens and this depends on the failure pressure and the extent of the weakened area of the wall. The maximum overpressure of this lead shock can be estimated using the 1D shock tube equation as will be shown later.

This lead shock travels at supersonic speed out into the surrounding atmosphere and it decays with distance. This is the



Fig. 3. Image of opened tube with flattened part still attached to ends. Failure runs along top of tube and then turns circumferentially at the ends of the weakened length.

moving lead shock produced by a BLEVE and it can do damage in the near and far field. There are many correlations available in the open literature (Casal and Salla, 2006; Genova et al., 2008; Planas-Cuchi et al., 2004; Prugh, 1991; Sellami et al., 2018) that can be used to predict the overpressure vs distance for the far field. Many of these correlations are based on the liquid energy in the vessel and then some factor is applied to adjust for the energy that actually goes into the shock wave. These can be used for the far field but they should probably not be used for the near field. Other models based on numerical simulations use the boiling dynamic of the fluid to determine the overpressure generated by the explosion (van den Berg et al., 2004; Hansen and Kjellander, 2016; Pinhasi et al., 2007; Yakush, 2016). Some ideal hypotheses are implemented to make the calculation possible, such as the vessel wall disappearing instantaneously, the two-phase fluid being in homogeneous equilibrium, and more. In reality it is questionable that the liquid energy is the source of the lead shock as will be argued in this paper.

While the lead shock is being generated the jet flow from the opening develops to become a choked sonic flow somewhere near the minimum opening area. This sonic jet continues to expand beyond the opening into a supersonic jet. This flow then goes through a normal shock (Mach shock) to reduce the flow back to subsonic velocity and a pressure more in line with the surroundings. This shock (Mach shock) as shown in Fig. 1 stands near the opening in the vessel wall. The barrel shock spreads from the sides of the opening to meet up with the Mach shock. The barrel shock marks the edge of the rapidly accelerating supersonic jet before it goes through the Mach shock to return to subsonic flow. We also see the edge of the jet interface behind the lead shock. The lead shock is generated by the expanding jet pushing on the surrounding air

like a piston. Compression waves generated by the piston produce the lead moving shock and it is sent out into the surroundings at supersonic speed. This standing Mach shock is not the lead shock that travels into the surroundings.

For a propane vapour release this standing shock is sometimes visible because condensation takes place in the region between the Mach shock and the edge of the jet interface. The condensation of the supersaturated vapour allows to visually locate the shock. Fig. 2 shows this standing shock above a fish mouth opening that has developed in a failing pressure vessel (0.4 m³) holding propane (Laboureur et al., 2015). The pressure profile on the left is derived from gas dynamic principles. The details of the profile definition can be found in the concerned paper.

Fig. 2 shows the pressure distribution along the axis of the jet leaving the vessel. The vapour accelerates along a streamline from the source pressure of P_0 to sonic velocity at P_1 . Then the vapour continues to accelerate to supersonic speed at P_2 where it then moves through a normal steady (stationary) shock (Mach shock) and the pressure jumps up to P_3 . This expansion happens so rapidly the vapour remains a supersaturated vapour until it passes through the shock which then triggers condensation. Beyond this the jet slows down and the pressure rises to meet the local pressure conditions.

At the same time the opening in the wall is growing with time and this affects the standing shock position and strength. At some point the vessel opens fully to release the vapour space. We are not sure when the vessel is fully open but from pipe rupture literature, it is defined to be when the open area is similar to the 2 x full cross sectional area of the vessel ($2A$) (Baum and Butterfield, 1979).

When the vessel fully opens we expect that the standing shock moves back into the vessel and disappears. This is similar to what happens with a choked converging-diverging nozzle when the source pressure decays. As the shock moves back into the throat the shock Mach number moves towards unity and then it goes subsonic.

Once the vessel is fully open and the pressure has decayed to some lower value the liquid will be in a metastable state of superheat. At this point the liquid begins to flash near the surface and a boiling wave is sent down into the liquid. The sudden phase change at this boiling wave generates a large thrust force as a two phase mixture is propelled upwards and outwards from the vessel. This downwards force causes a very large and brief ground loading. The expanding two phase flow also produces an overpressure (but not a shock wave) and drag force loading on nearby objects. During this phase where the liquid is flashing the vessel wall continues to open until it is flattened on the ground.

High speed imaging of a single step BLEVE suggests the liquid has little to do with this initial opening of the vessel and the production of the lead shock wave. This is strictly true only for the case of a single step BLEVE (a BLEVE where the vessel opening is very rapid). In a two-step BLEVE the growth of the opening stops at some point when the opening is quite small and is restarted by a pressure



Fig. 4. image of failed tube with separated part of wall flattened on blast plate. Weakened length is the upper and lower free edges of the flattened part.

transient in the vessel. This pressure transient is likely due to liquid flashing caused by the initial pressure drop as the opening started to grow.

1.3. Dimensional analysis

This dimensional analysis is based on the following assumptions:

- i) fluid viscosity is not an important factor in this analysis
- ii) important fluid properties include the liquid and vapour density, the surface tension, and the ratio of specific heats k of the vapour.
- iii) the lead shock overpressure is a function of how quickly the vessel opens and the volume and pressure-temperature of the vapour space.
- iv) the speed of this vessel opening is determined by the cut length, the tube wall thickness, and the failure pressure which is determined by the liquid temperature.
- v) the ground force depends on how quickly the vessel opens, the failure pressure, the tube size and the liquid fill level
- vi) the surface tension is included to acknowledge there may be a scale effect that we are not including with our small scale apparatus. However, it should be noted that similar processes and overpressures have been observed in vessels with diameters twenty times (volumes $1800/0.6 = 3000$ times) greater than in these experiments (Birk and VanderSteen, 2006)

The dimensional analysis has been conducted and suggests the following functional relationship for the blast overpressure and ground loading.

$$\frac{F_g}{P_f L D} = f \left[\frac{L}{D}, \frac{L_c}{L}, \frac{t_w}{D}, \text{fill}, \frac{T}{T_{sl}}, \frac{T}{T_{sat}}, \frac{\sigma d_d}{P_f D^2}, k, \frac{\rho_g}{\rho_f} \right] \quad (1)$$

$$\frac{dP_s}{dP_{st}} = f \left[\frac{L}{D}, \frac{L_c}{L}, \frac{t_w}{D}, \text{fill}, \frac{T}{T_{sl}}, \frac{T}{T_{sat}}, \frac{\sigma d_d}{P_f D^2}, \frac{R}{R_o}, k, \frac{\rho_g}{\rho_f}, \frac{P_f D}{2t_w \sigma_{yld}} \right] \quad (2)$$

where,

- D = tube diameter
 - d_d = vapour bubble or liquid droplet diameter
 - σ = surface tension
 - L = tube length
 - L_c = weakened cut length
 - t_w = tube wall thickness
 - fill = liquid fill fraction
 - T = liquid temperature
 - T_{sl} = atmospheric superheat limit temperature
 - T_{sat} = saturation temperature for failure pressure
 - P_f = failure pressure
 - dP_{st} = overpressure from 1D shock tube equation from P_f and T and $k = c_p/c_v$
 - dP_s = peak overpressure at R
 - R_o = radius of sphere with same volume as vapour space
 - σ_{yld} = yield strength of the tube material
- In this series of experiments, a number of these variables and groups were held constant (D, L, t_w , propane, k and d_d and $T/T_{sat} = 1$) and the equations simplify to:

$$\frac{F_g}{P_f L D} = f \left[\frac{L_c}{L}, \text{fill}, \frac{T}{T_{sl}} \right] \quad (3)$$

$$\frac{dP_s}{dP_{st}} = f \left[\frac{L_c}{L}, \text{fill}, \frac{T}{T_{sl}}, \frac{R}{R_o} \right] \quad (4)$$



Fig. 5. 0.4 m³ pressure vessel suffering a BLEVE. Failure runs along top of vessel and turns circumferentially at the ends. This vessel eventually flattened on the ground.



Fig. 6. 0.4 m³ pressure vessel after suffering a BLEVE. Failure runs.

2. Experimental setup

2.1. Apparatus

To study these details, we designed and manufactured a small scale apparatus that would allow us to record detailed images of the failure process and to measure overpressures very near to the vessel (within $R/R_{tube} = 0.175/0.25 = 7$). The objective was to have an apparatus with failure modes similar to large scale horizontal cylinders heated (weakened) at the top in the vapour space. It is very difficult and expensive to do such tests in large scale. The apparatus involved an aluminum tube with $D = 50$ mm and $L = 300$ mm. The apparatus and failure was designed to be representative of a cylinder failing and suffering a BLEVE at its top and centre. Figs. 3–6 show the failure of the small tubes compared to the failure of larger pressure vessels. Further details of this apparatus will be given later in the paper.

The apparatus was designed and constructed to study the early moments of a BLEVE in a weakened cylinder. The key design objectives were:

- i) make the vessel as large as possible but small enough to be financially feasible to do many tests
- ii) the failure mode should be similar to what is seen in practice with horizontal cylindrical pressure vessels
- iii) allow for variable L/D and weakened length L_c/D
- iv) allow for variable failure pressure P_f

This apparatus consisted of the following parts:

- i) aluminum tube (6061 T6 annealed to T0) with $D = 50$ mm and $L = 300$ mm with wall thickness 1.6 mm
- ii) top of the tube machined to reduce the wall thickness over length L_c to give desired failure pressure in the range 10–35 bar.
- iii) Swagelok end caps. One machined to accept fill and vent lines, two thermocouples (type K 1 mm diameter), pressure transducers (TC-Direct 716-072) and a high speed pressure transducer (PCB M101A02). The other end cap machined to have a 30 mm diameter window
- iv) electric heater machined to cover bottom 30% of tube surface
- v) cradle to hold tube in position
- vi) blast plate below tube supported on high speed load cells (PCB M202B)
- vii) pencil type blast gauges (PCB 137A23) at various positions
- viii) high speed video viewing window end, tube side and top (high speed cameras available: Phantom V711, V2512, VEO710 and Photron SA3)
- ix) High speed shadowgraph viewing side and end (same cameras)
- x) electric valves to allow for purging, fill and venting the tube

Fig. 7 shows a schematic of the apparatus. Further details of the apparatus can be found in (Eyssette, 2018).

2.2. Test procedure

The tests were conducted indoors in a large high ceiling, well ventilated lab. The test procedure was as follows

- i) the tube was assembled with the end caps and mounted in the cradle.
- ii) all instruments were connected and checked for operation.
- iii) the data acquisition systems were turned on and data was recorded.
- iv) the tube was purged of air using several fill and vent cycles with propane liquid.
- v) the tube was then filled with liquid propane to the desired fill condition.
- vi) the electric heater was then turned on to slowly heat the liquid until the tube failed (5–20 minutes heating).
- vii) the failure process was captured with high speed video and shadowgraph (Settles, 2001)

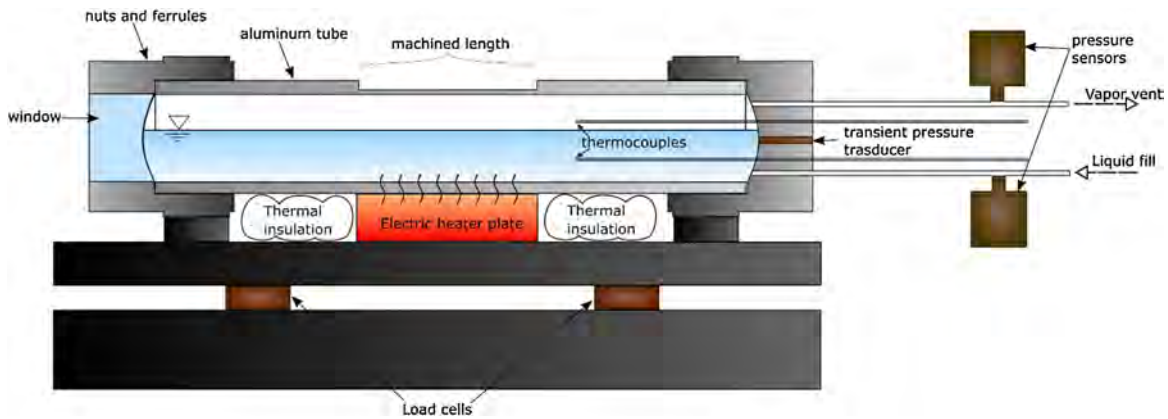


Fig. 7. Schematic diagram of tube apparatus (tube $D = 50$ mm).

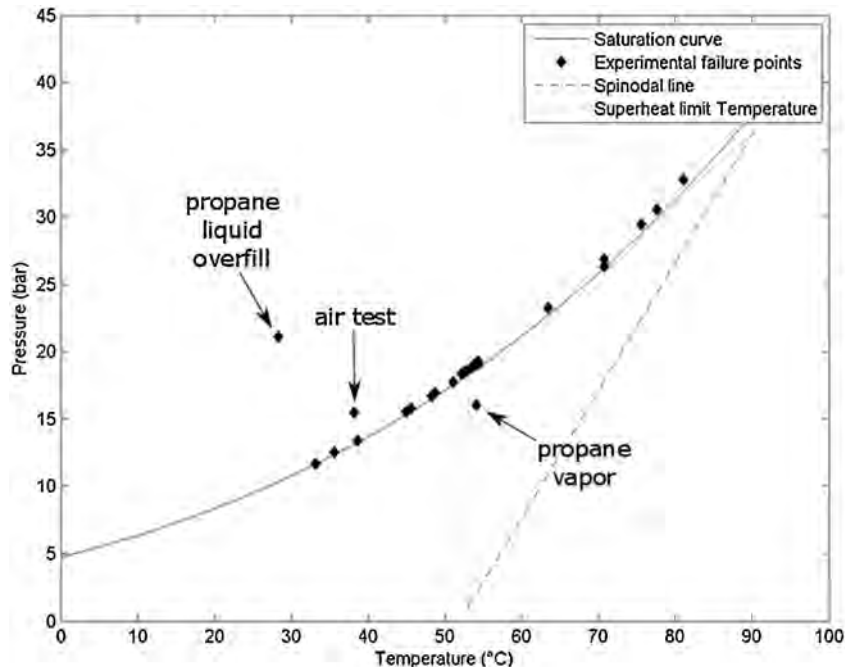


Fig. 8. Failure Temperatures and Pressures compared to saturation pressure curve for propane.

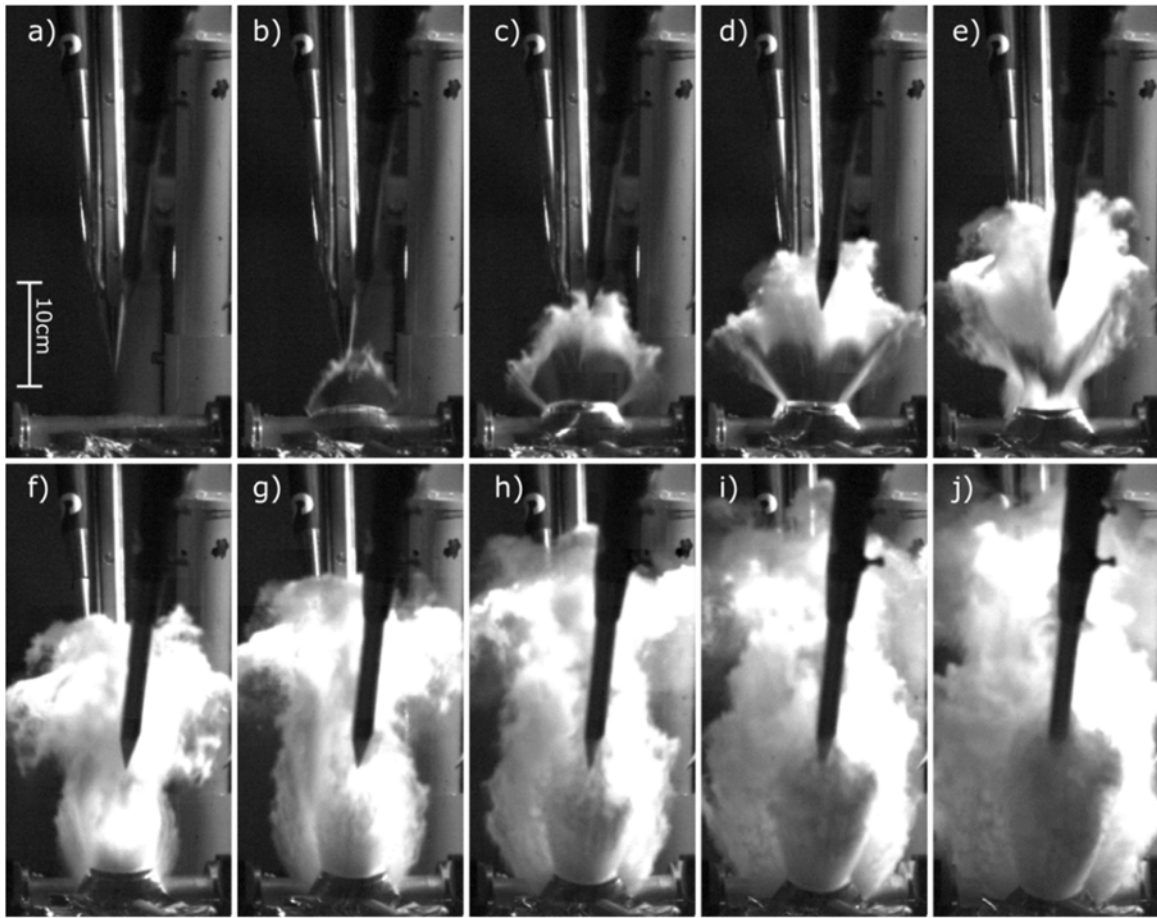


Fig. 9. Side view with direct high speed imaging (camera Photron SA3, $\Delta t = 200\mu s$, $P_f = 18.6bar$; fill = 56%; $L_c = 75mm$).

viii) all data was saved.

3. Results

The following results are shown here:

- i) liquid temperature saturation condition at failure
- ii) high speed images of vessel opening and formation of standing shock
- iii) high speed shadowgraph showing formation of lead shock
- iv) high speed imaging of top of vessel as wall opens showing liquid surface
- v) high speed imaging of window end showing boiling wave after the vessel is fully open (2 x-sect area)
- vi) peak overpressure vs distance showing location of formation of lead shock and decay of pressure following spherical shock theory

3.1. Failure pressure and liquid temperature

The tests were conducted over a range of failure pressures. This was done by machining the aluminum tubes to give the desired failure pressure. During each test the liquid propane was heated slowly until the tube failed when the von-Mises stress (0.866 hoop stress) in the tube wall was near the yield strength of the aluminum. Because of machining tolerances this method gave failure pressures within 10% of the desired failure pressure.

As can be seen from Fig. 8 almost all of the tests took place along the saturation curve for propane where the liquid and vapour are in

saturated equilibrium. This was desirable in this test to eliminate the one variable T/T_{sat} . This is not always the case in real world BLEVEs where there can be significant temperature stratification in the liquid and vapour space (Birk and Cunningham, 1996).

It is also important to note that the failure temperatures were below, at and above the atmospheric superheat limit for propane ($52^\circ C$). There were no extraordinary events when the T_{sl} was reached or exceeded. Of course the small scale may have had some effect on this. However similar results have been seen in much larger scales (volumes 3000 times larger) (Birk et al., 2006; Johnson and Pritchard, 1991).

3.2. High speed imaging and shadowgraph

The following figures show the early moments of the tube failure and the release of the vapour and liquid. Not all of the images are from the same test because we did not have enough equipment to do all views at the same time.

3.2.1. High speed imaging – side view

The example of high speed imaging of the tube side is from a test with the following conditions:

$$P_f = 18.6bar ; fill = 56% ; L_c = 75mm ; frame time step \Delta t = 0.2ms$$

One example of high speed imaging from a test is shown in Fig. 5. This example was chosen because it shows the creation of the standing shock and vapour condensation above the failure opening very clearly. Although it is not visible in these images, the lead shock was above the initial white cloud and quickly left the field of

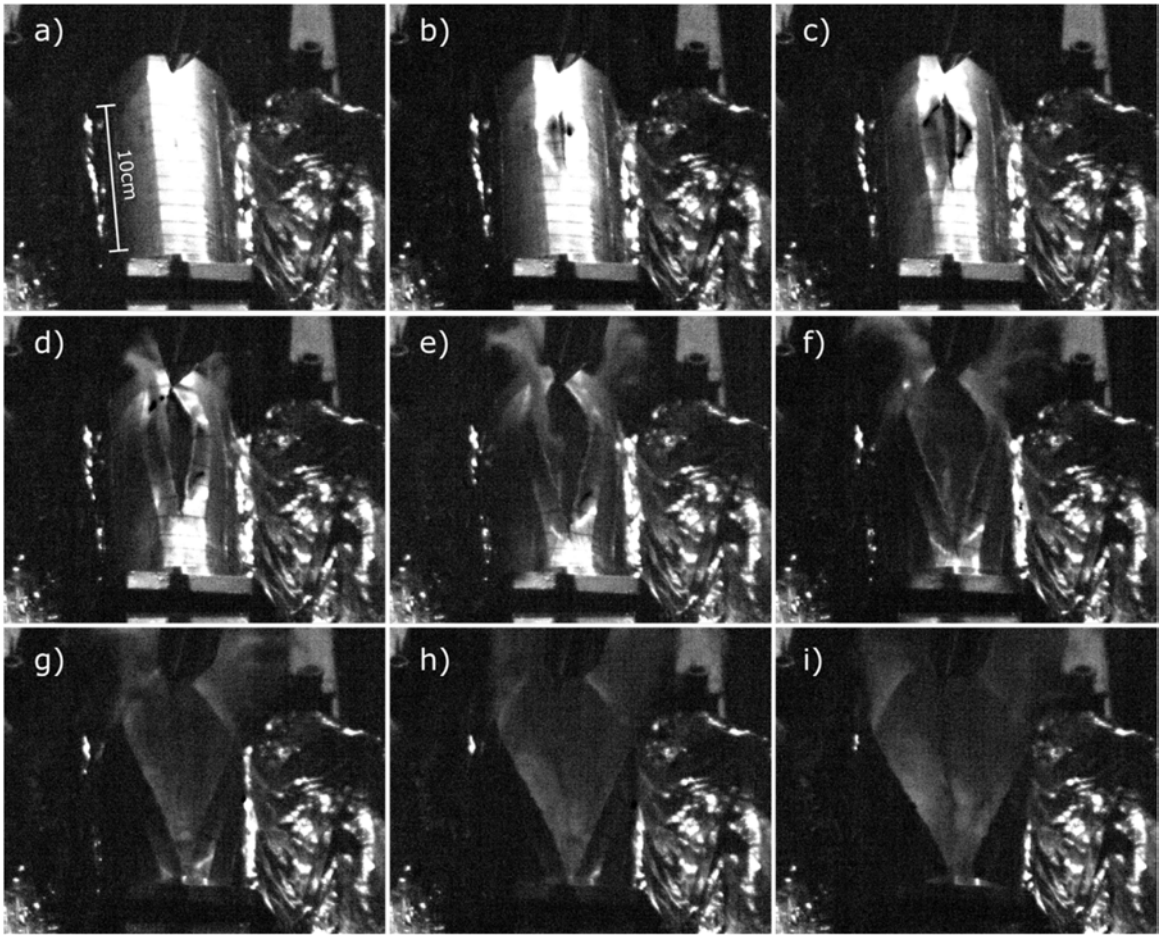


Fig. 10. Top view with direct high speed imaging (Camera Phantom VE0710, $\Delta t = 52\mu s$, $P_f = 19.3bar$; $fill = 84\%$; $L_c = 150mm$).

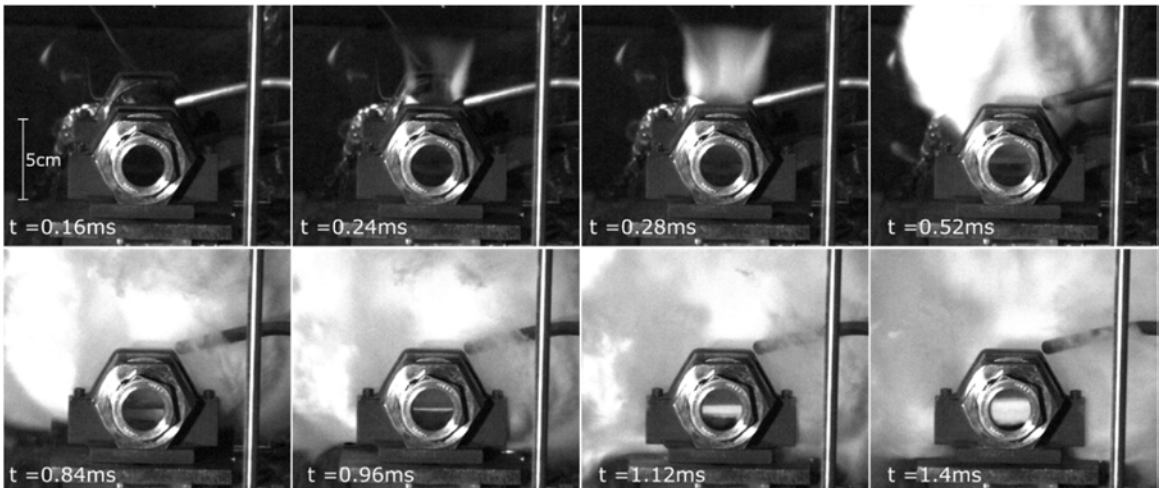


Fig. 11. Axial end view with direct high speed imaging (Camera Phantom V711, $P_f = 28bar$; $fill = 56\%$; $L_c = 75mm$).

view because it was moving much faster than the cloud. This will be shown in subsequent images.

In frame a) we see nothing because the failure opening has not started. By frame b) 0.2 ms later the opening has already grown the full length of the weakened length of 75 mm. In frames b), c) d) and e) the fish mouth opening is growing to fully open the vessel (open area greater than 2 x tube cross sectional area). In frames b) and c) you can clearly see the curved Mach shock

on the top with condensation of vapour trailing after the shock. You can also see the barrel shock on the sides leading from the ends of the fish mouth opening. By frame e) something has happened to both the Mach shock and barrel shock. The three dimensional aspect of the condensation cloud hides the top of the dome. However we think that the Mach shock is potentially collapsing and falling back into the throat as the pressure decays in the tube.

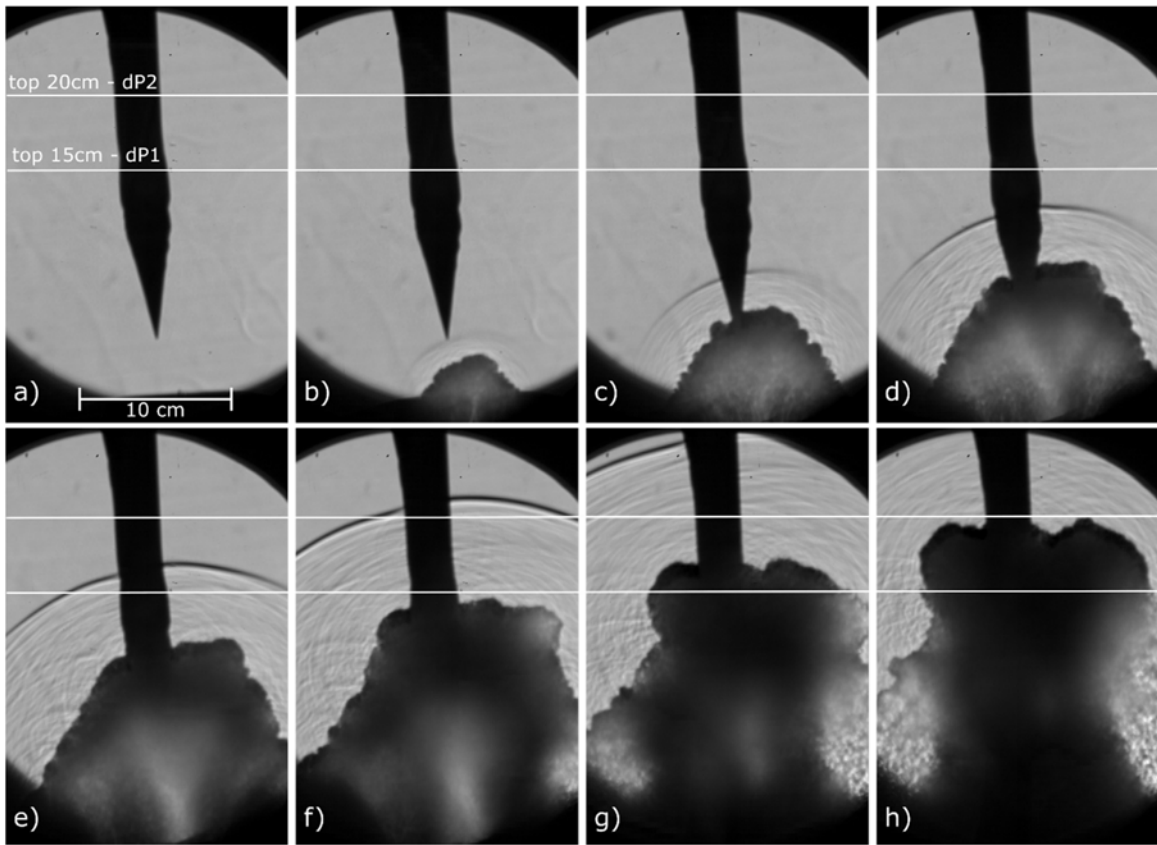


Fig. 12. Radial view with shadowgraph high speed imaging (Camera Phantom V2512, $\Delta t = 120\mu s$, $P_{fail} = 19.3\text{ bar}$, $\Phi_{liq} = 84\%$, $L_w = 150\text{ mm}$).

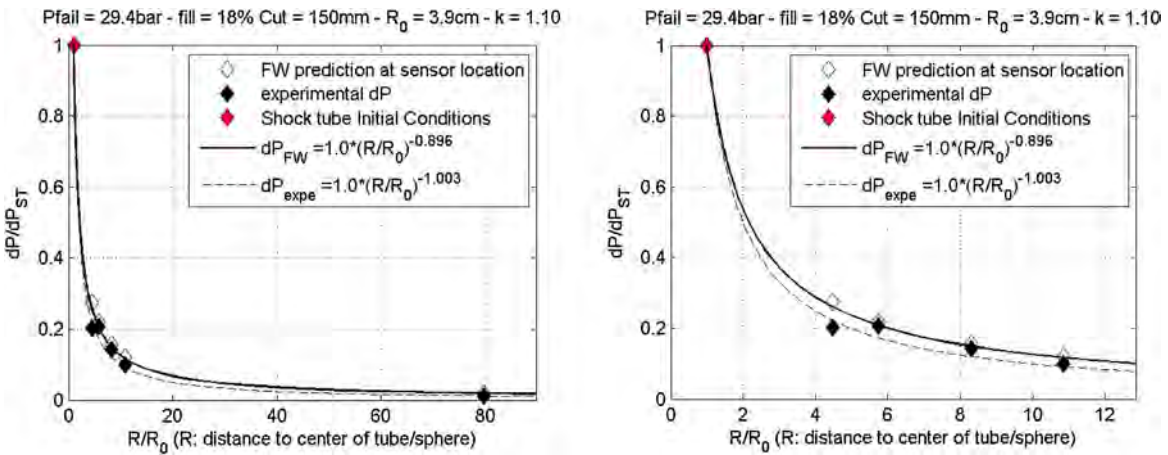


Fig. 13. Measured Peak Overpressure vs scaled distance R/R_o where R_o = radius of sphere based on vapour space volume along the tube weakened length (left: full scale along R/R_o ; right: zoom on the first 4 sensors).

The images also show the contribution of the vapour space and the liquid space. The first small ball of white cloud (image e) is the vapour space. Then behind this you see a second cloud which is the liquid flashing. This you can see starting somewhere between frame e) and f) and continuing into frame j). The lead shock is long gone by this time.

It is the propane interface (the first white cloud from the vapour) that acts as the piston to start the lead shock.

3.2.2. High speed imaging – top view

The next sequence of images shows the top view. The test details for this case were

$P_f = 19.3\text{ bar}$; $fill = 84\%$; $L_c = 150\text{ mm}$; $frame\ time\ step\ \Delta t = 0.052\text{ ms}$

In Fig. 10: frame a) we see the pin hole forming on the machined flat area. The crack reaches the end of the machined part ($L_c = 150\text{ mm}$) by frame g) or about 0.31 ms. At this point the tube

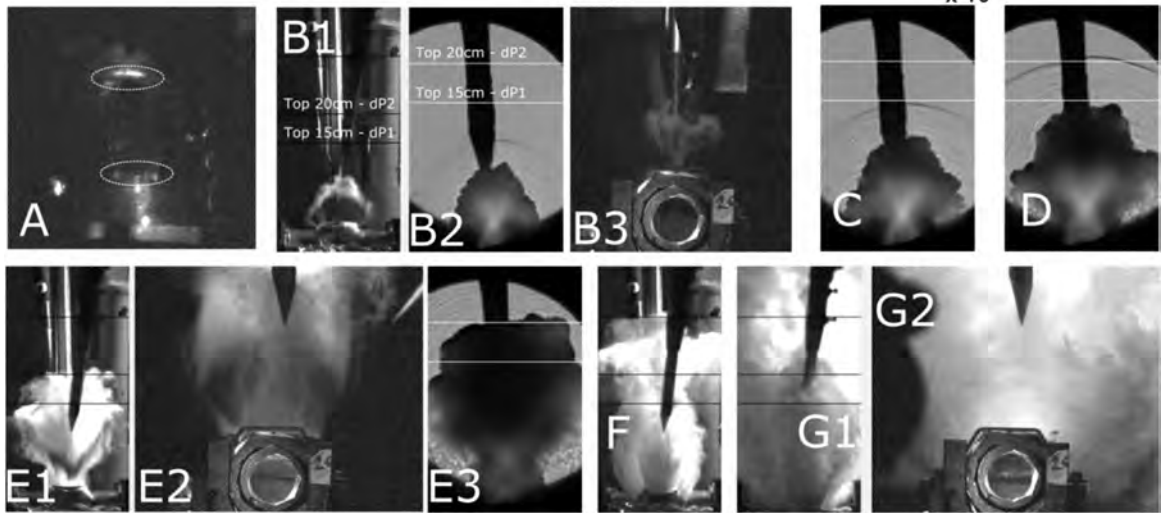
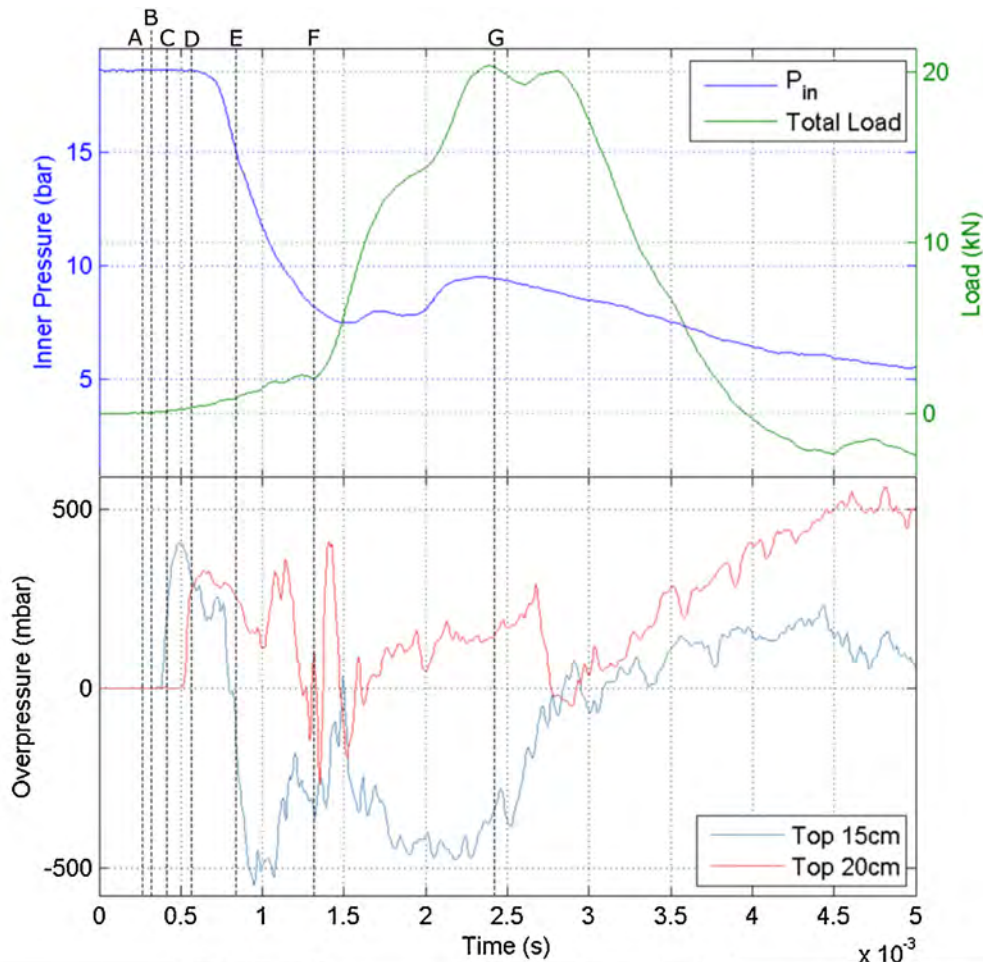


Fig. 14. Chronology of a BLEVE through physical measurements and high speed imaging ($P_{fail} = 18.6\text{bar}$, $\Phi_{liq} = 56\%$, $L_w = 75\text{mm}$).

is almost fully open (i.e. the open area is greater than 2 x cross sectional area of the vessel). The lead shock has been sent out into the surroundings by this time. The tube is not flattened on the ground at this time. In frames d) and f) you can see some condensation on either side of the lips of the fish mouth opening. In the final frames we see the liquid surface in the vessel. There seems to be some convective patterns on the surface but bulk flashing has not begun. This suggests that the liquid has little to do with the lead shock.

3.2.3. High speed imaging – window end view

In this case the high speed video is viewing the window end of the vessel. The test details for this case are:

$$P_f = 28\text{bar}; \text{fill} = 56\%; L_c$$

$$= 75\text{mm}; \text{frame time step variable, shown on figure}$$

From Fig. 11 we can see from the end view that there seems to be little or no boiling activity up to around 0.28 ms. Then we see

some boiling takes place near the centre of the vessel at 0.52 ms. The tube is well opened by 0.28 ms suggesting the lead shock has left the cylinder. The boiling wave becomes a sharp boiling line at the window location by 0.96 ms. This suggests the boiling has reached the window location. Then we see the boiling wave grow downwards at the window in the final two frames. The boiling wave is moving down at a speed of around 25–30 m/s.

3.2.4. High speed shadowgraph –side view

The high speed shadowgraph is from a different test with the following test conditions:

$$P_f = 19.3 \text{ bar}; \text{fill} = 84\%; L_c = 150 \text{ mm}; \text{frame time step } \Delta t = 0.052 \text{ ms}$$

The high speed shadowgraph is shown in Fig. 8 and it clearly shows the creation of the lead shock above the cloud of expanding vapour propane. The cloud shows the interface between the surrounding air and the released vapour propane. The image also shows the position of the first two blast gages mounted directly above the tube at 15 and 20 cm from the tube upper surface (17.5 and 22.5 cm from tube centre).

In frame a) the tube is just beginning to fail and no release is visible. In frame b) we can clearly see the vapour coming out and acting as a piston to push the surrounding air out of the way. Still in frame b) we see a hint of a shock forming above the cloud. The lead shock continues to build in strength until it reaches full strength somewhere around frame e) and f). We know this because in some cases the overpressure is greater for the second blast gage (at 20 cm) than the first blast gage (at 15 cm). This suggests the overpressure has increased as the shock fully forms. Once the shock is fully formed it begins to decay as it travels at supersonic speed into the surroundings.

3.3. Measured peak overpressure vs distance

The data shown here is from a test with the following details:

$$P_f = 29.4 \text{ bar}; \text{fill} = 18\%; L_c = 150 \text{ mm}$$

Fig. 9a) shows the measured peak overpressure vs the scaled distance from the test. The distance is scaled by R_0 which is the radius of a sphere with a volume equal to the vapour space volume along the cut (weakened) length of the tube.

As can be seen the overpressure is larger for the position at $R/R_0 = 6$ than it is at $R/R_0 = 4.5$. This suggests the shock continued to build strength until $R/R_0 = 6$. The solid line is the predicted shock strength based on the Friedman-Whitham theory for a spherical shock (Kornegay, 1965). The starting overpressure for this model is based on the 1D shock tube equation using the failure pressure and temperature and $k = c_p/c_v = 1.1$ for the propane. As can be seen the measured overpressure does not agree with F-W theory until the shock is fully formed at around $R/R_0 = 6$.

Fig. 13 (right) shows the scale expanded to $R/R_0 = 80$. We see that the measured pressure decays slightly faster than that predicted by F-W.

This model for the lead shock does not include any kind of energy calculation. It is based on the failure pressure and temperature and the volume of the vapour space under the weakened part of the wall. We did not apply any factors to reduce the fraction of energy that went into the formation of the shock. The full set of experimental data is currently being analyzed using this method and will be published when available.

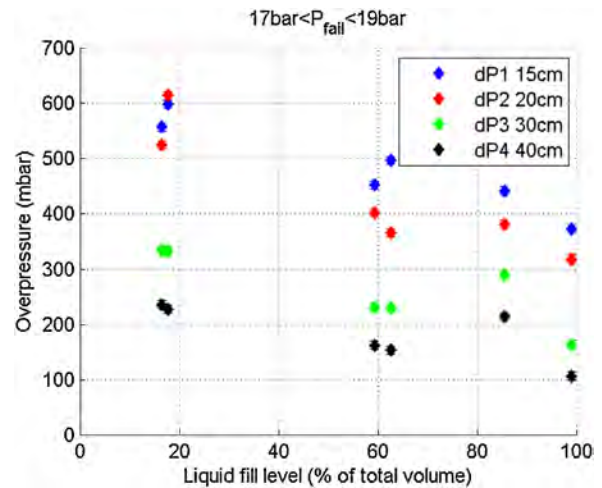


Fig. 15. Maximum overpressure measured above the vessel at 4 different distances, against liquid fill level, for cases of similar failure pressure ($17 \text{ bar} < P_{\text{fail}} < 19 \text{ bar}$) and cut length (150 mm).

4. Discussion

4.1. Chronology of a BLEVE: sample case

This sample case is presented to identify specific milestones in the opening of the vessel. All the data is from the same test with the following details

$$P_f = 18.6 \text{ bar}; \text{fill} = 56\%; L_c = 75 \text{ mm}$$

The exact timing of these milestones varied from test to test and depended on the tube fill level, the length of the weakened zone and on the liquid temperature at failure (i.e. failure pressure).

These milestones are described with the aid of Fig. 14 which shows the time plots of the overpressures measured near the top of the tube and by the ground loading. Fig. 14 also shows images that illustrate these key events.

The milestones are:

- i) start of the opening process ($t = 0 \text{ s}$) with uncertainty of around 0.1 ms.
- ii) failure crack grows to the ends of the machined length (one or two frames or $0.3 \text{ ms} \pm 0.1 \text{ ms}$, speed = 94 – 188 m/s)
- iii) failure fully opened (open fish mouth area $\geq 2 \times$ tube cross section area) (0.5 ms)
- iv) lead shock reaches first blast sensor above tube (0.5 ms at distance of 0.15 m from tube surface $R/R_{\text{tube}} = 7$)
- v) ground loading begins due to vapour release (0.5 ms)
- vi) lead shock reaches second blast sensor above tube (0.7 ms at 0.2 m)
- vii) pressure begins to drop at transducer location in tube end (0.68 ms) (time for depressurization wave to traverse half tube length)
- viii) second white cloud from liquid begins (0.8 – 0.9 ms)
- ix) liquid boiling wave observed to start (after 0.8 – 0.9 ms)
- x) sudden change in slope of ground loading curve (1.3 ms)
- xi) first pressure minimum in tube (1.5 ms)
- xii) pressure recovery (from liquid flashing) in tube begins (1.5 ms)
- xiii) peak of pressure recovery in tube (2.3 ms)
- xiv) tube flattened on ground (2.4 ms)
- xv) peak ground loading (2.4 ms)
- xvi) ground loading ends (4.5 ms)
- xvii) pressure in tube returns to ambient level ($> 5 \text{ ms}$)

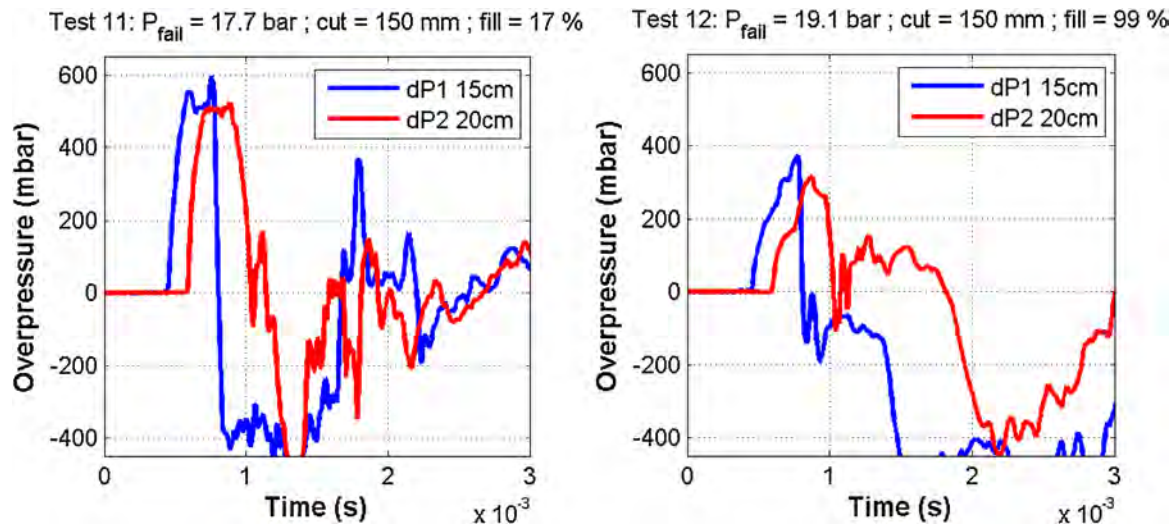


Fig. 16. Pressure signals from two sensors above the vessel (15 and 20 cm) for two cases of similar failure pressure and cut length, but different liquid fill level.

The time origin $t=0$ s was chosen to be the time at which the vessel starts to open. All of the above times that are based on images have some uncertainty associated with them of around 0.1 ms which was half the frame rate 0.2 ms of the camera. Times based on measured pressures have a much lower uncertainty of around 0.01 ms.

A key observation is that the process of the vapour release and lead shock production took around 0.5 ms while the liquid effects start at around 0.8 ms. The powerful liquid flashing process lasts for around 4 ms, almost an order of magnitude greater than the vapour effects.

Another key observation is the relatively small pressure recovery in the vessel when the liquid started strong flashing. This was because the event was a single-step BLEVE where the vessel was fully open when the liquid flashing was triggered. In a two-step BLEVE we would expect a larger pressure recovery because the opening would be only partially formed (Birk et al., 2007).

4.2. Contribution to the lead shock

Chronology (Fig. 14) and high speed imaging (Fig. 12) show that the lead shock is synchronized with vapour expansion. The liquid boiling does not seem to contribute to the lead shock overpressure, because the shock is long gone before the liquid starts to boil. Experiments show a correlation between the maximum overpressure and the vapour content in the vessel before failure (Fig. 15).

Moreover, the pressure signals show that on top of having weaker maximum overpressure, the steepness of the overpressure itself decreases with increasing liquid content in the vessel, to a point where it cannot be called a shock anymore (Fig. 16 right). The authors do not state that the liquid boiling does not generate overpressure. It does in most cases, after the initial lead shock has propagated away from the vessel. However, it does not contribute to the first overpressure measured or predicted as the maximum overpressure.

For cases with 100% liquid in the vessel, the lead shock cannot come from the vapour phase expansion, thus overpressure generated by the liquid boiling must be considered.

Experiments from the literature report strong overpressures from BLEVE with propylene full of liquid at failure (Giesbrecht et al., 1981). However, no pressure trace is available in this reference. Thus it is not clear if these overpressure are steep shocks or more progressive overpressure, as shown Fig. 16 right.

Some simulation work models the overpressure generated by a BLEVE with a full liquid vessel as initial condition. One study shows that for cases with high failure pressure and temperature, shocks are observed as a result of the release of the pressurized content (Pinhasi et al., 2007). Stronger failure pressure lead to stronger evaporation rate, thus stronger overpressure build-up, which could potentially lead to shock formation for strong enough failure conditions. However, this result has not been validated with experiment. Other simulation works lead to shock generation from the evaporation of pressurized liquid content (van den Berg et al., 2004; Yakush, 2016). However they are based on ideal conservative assumptions:

- i) Instantaneous disintegration of the vessel wall: the pressure drop rate in the vessel is at its maximum, which is not the case for experiments where the vessel walls take some time to get out of the way of the expanding gas (approximately 0.5 ms for full opening, 2.5 ms for flat tube on the ground for our experiments)
- ii) Instantaneous intrinsic evaporation of the superheated liquid: this means there is no delay due to the metastable aspect of the superheat before nucleation triggers the boiling, and the evaporation rate does not depend on the bubble size growth rate, solely on extrinsic circumstances (gas dynamic, presence of surrounding atmosphere to be pushed away)

The discussion on the contribution of the liquid in the main overpressure if no vapour phase is present revolves around the validity of these assumptions, which are never as ideal in reality, guiding the vapour release rate and the expansion of the two-phase mixture. More experiments with full liquid vessel burst are required to conclude on the argument of the shock generation by the boiling liquid.

5. Conclusions

The following conclusions have been made based on the data presented.

- i) the vessel failures in this study were single-step BLEVEs where the vessel failure process was rapid and continuous
- ii) the vessel failures were due to the von Mises stress based on the measured tube pressure exceeding the tube material yield strength. There was no internal pressure transient (BLEVE in tube) that triggered the tube failure.

- iii) no extraordinary events were observed when the liquid was at or above the atmospheric superheat limit.
- iv) The results suggest the lead shock is due to the vapour space and that the liquid does not contribute significantly to this process.
- v) the lead shock is fully formed somewhere between $R/R_{tube} = 7-9$ for the case of the 18.6 Barg failure with liquid fill = 56% and weakened length of 75 mm
- vi) The liquid flashing does not appear to produce its own shock because of the slower release process.
- vii) the pressure recovery in the vessel was small because this BLEVE was a single step and the vessel was fully open when the liquid flashing began.
- viii) the liquid flashing process is one order of magnitude slower than the vapour release.
- ix) The ground loading is dominated by the liquid flashing process.

Declaration of Competing Interest

None.

Acknowledgments

This work was a collaboration between the Mechanical and Material Engineering of Queen's University in Canada and the LGEI at IMT Mines Alès in France. It was possible thanks to the funding from the Natural Sciences and Engineering Research Council of Canada with a discovery grant.

References

Abbasi, T., Abbasi, S.A., 2007. *J. Hazard. Mater.* **141**, 489–519.

- Baum, M.R., Butterfield, J.M., 1979. *J. Mech. Eng. Sci.* **21**, 253–261.
- van den Berg, A.C., van der Voort, M.M., Weerheijm, J., Versloot, N.H.A., 2004. *J. Loss Prev. Process Ind.* **17**, 397–405.
- Birk, A.M., Cunningham, M.H., 1996. *J. Hazard. Mater.* **48**, 219–237.
- Birk, A.M., Davison, C., Cunningham, M., 2007. *J. Loss Prev. Process Ind.* **20**, 194–206.
- Birk, A.M., Poirier, D., Davison, C., 2006. *J. Loss Prev. Process Ind.* **19**, 582–597.
- Birk, A.M., VanderSteen, J.D.J., 2006. *Trans. ASME* **128**, 648–655.
- Casal, J., Salla, J.M., 2006. *J. Hazard. Mater.* **137**, 1321–1327.
- Eckhoff, R.K., 2014. *J. Loss Prev. Process Ind.* **32**, 30–43.
- Eyssette, R., 2018. *Characterization and Modeling of Near-field BLEVE Overpressure and Ground Loading Hazards*. Queen's University(Canada) / IMT Mines Ales, France.
- Genova, B., Silvestrini, M., Leon-Trujillo, F.J., 2008. *J. Loss Prev. Process Ind.* **21**, 110–117.
- Giesbrecht, H., Hess, K., Leuckel, W., Maurer, B., 1981. *Ger. Chem. Eng.* **4**, 315–325.
- Hansen, O.R., Kjellander, M.T., 2016. **48**, 199–204.
- Hemmatian, B., Casal, J., Planas, E., Rashtchian, D., 2019. *J. Loss Prev. Process Ind.*
- Johnson, D.M., Pritchard, M.J., 1991. *A Large Scale Experimental Study of BLEVEs*. British Gas Report No 1536, United Kingdom.
- Kornegay, W.M., 1965. *Distribution 1965. Production and Propagation of Spherical Shock Waves at Low Ambient Pressures*.
- Laboureur, D., Birk, A.M., Buchlin, J.M., Rambaud, P., Aprin, L., Heymes, F., Osmont, A., 2015. *Process Saf. Environ. Prot.* **95**, 159–171.
- Laboureur, D., Heymes, F., Lapebie, E., Buchlin, J.M., Rambaud, P., 2014. *Process Saf. Prog.* **33**, 274–284.
- Pinhasi, G.A., Ullmann, A., Dayan, A., 2007. *Int. J. Heat Mass Transf.* **50**, 4780–4795.
- Planas-Cuchi, E., Salla, J.M., Casal, J., 2004. *J. Loss Prev. Process Ind.* **17**, 431–436.
- Prugh, R.W., 1991. *J. Fire Prot. Eng.* **3**, 9–24.
- Radulescu, M.I., Law, C.K., 2007. *J. Fluid Mech.* **578**, 331–369.
- Sellami, I., Nait-Said, R., de Izarra, C., Chetehouna, K., Zidani, F., 2018. *Process Saf. Environ. Prot.*
- Settles, G.S., 2001. *Schlieren and Shadowgraph Techniques: Visualizing Phenomena in Transparent Media*. Springer-Verlag, Berlin.
- Vigilfuoco.tv, [WWW Document]. URL 2018. BOLOGNA (BO) Loc. Borgo Panigale - Esplosione autocisterna. <http://www.vigilfuoco.tv/emilia-romagna/bologna/bologna/esplosione-autocisterna>.
- Yakush, S.E., 2016. *Int. J. Heat Mass Transf.* **103**, 173–185.